of the π_1 orbital (Table X), the effect of the p_y mixing is stronger than that of steric shielding for $CH_3C_6H_4Cl$ and $CH_3C_6H_4Br$ ($I(\pi_1)/I(\pi_2)$ = 1.41 and 1.18, respectively). However, the small $I(\pi_1)/I(\pi_2)$ value of 0.78 for $CH_3C_6H_4I$ shows that the shielding effect is predominant in this case owing to the effect of the large iodine atom and the weak π-n interaction.

3. Reactivities of σ Orbitals. The intensities of the σ bands also vary among the compounds. As shown below, this indicates that the shielding effect is largely affected by the size and position of the halogen atom. Table X shows the ratio of the average intensity of the σ bands to that of the π and n bands, $I(\sigma)/I(\pi,n)$, where $I(\sigma)$ denotes the average value of the intensities of the nine σ bands, $\sum I(\sigma)/9$, and $I(\pi,n)$ denotes that of the three π and two n bands, $[\sum I(\pi) + \sum I(n)]/5$. As is seen in Table X, the above ratio decreases in the order Cl derivatives > Br derivatives > I derivatives. This is because the size of the halogen lone-pair orbital becomes larger in the order, Cl(3p) < Br(4p) < I(5p), and hence the shielding effect on the σ orbitals becomes more significant from chloro to iodo derivatives.

The position of the halogen atom also influences the σ band intensity; the σ band in the para derivatives is much smaller than that in the ortho and meta derivatives (Table X). In the para derivatives, the methyl group and the halogen atom are separated from each other so that both of them effectively shield the σ orbitals from the attack of metastable atoms. On the other hand, in the ortho derivatives, the methyl group and halogen atom partly counteract their shielding effects on each other because their positions of substitution are adjacent. Thus, the shielding effect increases, and hence the relative intensity of the σ bands decreases in the order o > m > p. Such a shielding effect is also found in dichlorobenzenes.[10]

Conclusion

In Penning ionization electron spectroscopy (PIES), information is directly provided on the electron distributions of individual molecular orbitals of the molecule. On the basis of this unique feature of PIES, all the bands in the He I spectra of halogenotoluenes, *o*-, *m*-, and *p*-$CH_3C_6H_4X$ (X = Cl, Br, I), have been assigned. The band intensities in PIES are closely related to the reactivities of individual molecular orbitals. From the analysis of the band intensities of the halogenotoluenes, the reactivities and stereochemical properties of the n, π, and σ orbitals have been investigated. It was found that the orbital reactivities depend on the size of the halogen lone-pair orbitals, the interaction between the π and n orbitals, and also on the steric shielding effect of some orbitals against the attack of metastable atoms.

Registry No. *o*-$CH_3C_6H_4Cl$, 95-49-8; *m*-$CH_3C_6H_4Cl$, 108-41-8; *p*-$CH_3C_6H_4Cl$, 106-43-4; *o*-$CH_3C_6H_4Br$, 95-46-5; *m*-$CH_3C_6H_4Br$, 591-17-3; *p*-$CH_3C_6H_4Br$, 106-38-7; *o*-$CH_3C_6H_4I$, 615-37-2; *m*-$CH_3C_6H_4I$, 625-95-6; *p*-$CH_3C_6H_4I$, 624-31-7.

Absorption Spectrum of the Solvated Electron in Ammonia and Amines

Halina Abramczyk* and Jerzy Kroh*

Institute of Applied Radiation Chemistry, Technical University, 93-950 Łódź, Wróblewskiego 15, Poland
(Received: October 10, 1990)

The absorption spectra of solvated electrons in ammonia, methylamine, and trimethylamine are calculated in terms of the theory presented in our previous paper[1] and compared with the experimental data. The theory reproduces very well the experimental absorption spectra, their bandwidths, and the band shapes with the characteristic asymmetric tail on the high-frequency side. The role of the H bond in stabilization and spectroscopic properties of the solvated electron in amines are discussed.

Introduction

The nature of the solvated electron in ammonia and amines has been the subject of many experimental[2-19] and theoretical[20-29] studies, molecular dynamics simulations,[30-32] and ab initio calculations.[33-35] Ammonia is one of the most frequently studied

(1) Abramczyk, H. *J. Phys. Chem.*, in press.
(2) Dye, J. L.; Debacker, M. G.; Dorfman, L. M. *J. Chem. Phys.* **1970**, *52*, 6231.
(3) Jou, F.-Y.; Freeman, G. R. *Can. J. Chem.* **1979**, *57*, 591.
(4) Olinger, R.; Schindewolf, U.; Gaathon, A.; Jortner, J. *Ber. Bunsen-Ges. Phys. Chem.* **1971**, *75*, 690.
(5) Olinger, R.; Schindewolf, U. *Ber. Bunsen-Ges. Phys. Chem.* **1971**, *75*, 693.
(6) Jou, F.-Y.; Freeman, G. R. *J. Phys. Chem.* **1981**, *85*, 629, 633.
(7) Dealaire, J. A.; Barouin, J. R. *Can. J. Chem.* **1979**, *57*, 2013.
(8) Gavlas, J. F.; Jou. F. Y.; Dorfman, L. M. *J. Phys. Chem.* **1974**, *78*, 2631.
(9) Rubinstein, G.; Tuttle, T. R.; Golden, G. *J. Phys. Chem.* **1973**, *77*, 2872.
(10) Farhataziz; Perkey, L. M.; Hentz, R. R. *J. Chem. Phys.* **1974**, *60*, 4383.
(11) Seddon, W. A.; Fletcher, J. W.; Sopchyshyn, F. Ch. *Can. J. Chem.* **1978**, *56*, 839.
(12) Seddon, W. A.; Fletcher, J. W.; Sopchyshyn, F. C. *Chem Phys.* **1976**, *15*, 377.
(13) Fletcher, J. W.; Seddon, W. A.; Jevcak, J.; Sopchyshyn, F. C. *Chem. Phys. Lett.* **1973**, *18*, 592.
(14) Lin, D. P.; Kevan, L. *J. Chem. Phys.* **1971**, *55*, 2629.
(15) Farhataziz; Perkey, L. M. *J. Phys. Chem.* **1975**, *79*, 1651.
(16) Jou, F.-Y.; Freeman, G. R. *Can. J. Chem.* **1982**, *60*, 1811.
(17) Huppert, D.; Rentzepis, P. M.; Struve, W. S. *J. Phys. Chem.* **1975**, *79*, 2850.
(18) Shida, T.; Iwata, S.; Watanabe, T. *J. Phys. Chem.* **1972**, *76*, 3683.
(19) Haberland, H.; Langosch, H.; Schindler, H. G.; Worsnop, D. R. *Ber. Bunsen-Ges Phys. Chem.* **1984**, *88*, 270.
(20) Stupak, C.; Tuttle, T. R., Jr.; Golden, S. *J. Phys. Chem.* **1984**, *88*, 3804.
(21) Stupak, C.; Tuttle, T. R., Jr.; Golden, S. *J. Phys. Chem.* **1982**, *86*, 327.
(22) Tuttle, T. R., Jr.; Golden, S.; Lwenje, S.; Stupak, C. *J. Phys. Chem.* **1984**, *88*, 3811.
(23) Ogg, R. A. *J. Am. Chem. Soc.* **1946**, *68*, 155.
(24) Kestner, N. R.; Jortner, J. *J. Phys. Chem.* **1973**, *77*, 1040.
(25) Fueki, K.; Feng, D. F.; Kevan, L. *J. Am. Chem. Soc.* **1973**, *95*, 1398.
(26) Kajiwara, G.; Funabashi, K.; Naleway, C. *Phys. Rev. A* **1971**, *6*, 808.
(27) Kestner, N. R. In *Electron-Solvent and Anion Solvent Interactions*; Kevan, L., Webster, B., Eds.; Elsevier: Amsterdam, 1976; Chapter 1.
(28) Huang, J. T.; Ellisson, F. O. *Chem. Phys. Lett.* **1974**, *28*, 189.
(29) Jortner, J. *Ber. Bunsen-Ges. Phys. Chem.* **1971**, *75*, 696.
(30) Barnett, R. N.; Landman, U.; Nitzan, A. *J. Chem. Phys.* **1989**, *91*, 5567.
(31) Sprik, M.; Klein, M. L. *J. Chem. Phys.* **1988**, *89*, 1592.
(32) Sprik, M.; Klein, M. L. *J. Chem. Phys.* **1989**, *91*, 5665.
(33) Newton, M. D. *J. Phys. Chem.* **1975**, *79*, 2795.

0022-3654/91/2095-5749$02.50/0

media for the stabilization of the excess electron and together with water provides the model example of the classical many-body system coupled to a quantum system undergoing the fluctuations of the solvent. Both solvents as liquids, glasses, and solid crystals consist of polymeric species associated by H bonding.[36-38] Despite much experimental and theoretical interest, the influence of H bonding on localization, electron attachment, stabilization, solvation, dynamics of localization, and spectroscopic properties in bulk liquid ammonia and water as well as in small clusters remains unclear. The theoretical calculations should help us find the sites of preferential attachment within a molecular cluster and learn whether an electron (a) enters a cavity and remains in the center, through breaking the existing H-bond structure, (b) attaches to preexisting groups of molecules with free OH or NH bonds, or (c) does not break the H-bond structure being attached as an additional electron in the diffuse solvent anionic complex.

In order to answer these questions, three main structures have been considered for H-bonded solvents: (a) the electron localized in a cavity,[23,33,34,39-44] (b) the solvated diffuse anionic complex,[45-51] and (c) the polaron.[52] Structures with the electron in a cavity are currently most favored, but the questions remain, what is the structure of the cavity, what are the sites of preferential attachment within a molecular cluster? In the framework of the cavity models, dipole-oriented[33,53,54] and H-bond-oriented[30-32,55-57] structures have been considered for H-bonded solvents.

Alcohols seem to ignore the H bond in creating the dipole-oriented cavity.[53] On the contrary, H-bond-oriented cavities seem to exist in water, ammonia, and amines.[30-32,34,55-57] Experimental electron spin resonance results,[39] molecular dynamics simulations, and some ab initio calculations[31-33,35,49-51] suggest that six protons in OH or NH bonds are directed toward the electron localized at the center of a cavity of $(H_2O)_6^-$ or $(NH_3)_6^-$. The results of Newton[33] showed that the cavity seems to be formed by free OH or NH groups, and fully H-bonded molecules do not appear to offer especially favorable trapping sites. The theoretical calculations are consistent with nozzle beam studies[58] where the increase in signal intensity at $n = 6$ is observed. However, most unexpected is the detection of dimers $(H_2O)_2^-$[58] because it seems that only larger clusters are required both for water and ammonia[19] for trapping an electron. Despite ab initio results for an electron in negatively charged clusters, which strongly depend on the diffuseness of the basis set, we can notice a few quite marked differences in the structures of hydrated and ammoniated electrons: (a) the size of a cavity for NH_3 is calculated to be 3.9 Å, while for water 2.6 Å;[33] (b) the breathing mode force constant of an e_{am}^- cavity is markedly smaller than that of an e_{aq}^- one; (c) an ammoniated electron is calculated to be appreciably less strongly bound or even unbound relative to an isolated electron and six ammonia molecules;[33] (d) electron spin density on protons in water is positive while in ammonia it is negative;[33,34,54] and (e) ammonia clusters of any size do not form well-bound excess electron surface states, resulting in the onset of electron binding via internal localization for $n \geq 32$.[30]

The second problem is the role of H-bond interactions in the dynamics of electron localization and stabilization. Technological advances in the creation and detection of ultrashort optical pulses have made it possible to study the nearly first stage of the time evolution of electron localization.[59] An alternative approach is molecular dynamics simulations.[30-33] Barnett, Landman, and Nitzan[30] have investigated by molecular simulation experiments very early stages following excess electron injection in ammonia and water. They start from a system in which an electron is initially attached to an equilibrated neutral cluster in the ground electronic state in the preexisting trapping sites[60-64] due to the process of multiphonon nonradiative transitions[65] or as a result of charge-induced polarization.[66-68] H-bond interactions play a role in the first stage of the dynamics of excess electron migration (0.15–4 ps for ammonia clusters and 0.15–1.2 ps for water) during reorganization in the vicinity of the electron with NH or OH bonds pointing toward the excess electron as a final result. In the next step, migration of the electron toward the center of the cluster occurs, characterized by polaron-like dynamical evolution. The processes of excess electron migration are slower in ammonia than in water. The question arises, what is the major interaction responsible for the equilibrium structures suggested by MD and electron spin resonance spectra of the solvated electron in H-bonded solvents? Clark and Illing[34] suggest that the major interaction, apart from spin polarization, is hydrogen bonding with the localized electron as a donor to the antibonding σ_{OH}^* or σ_{NH}^* orbitals in water and ammonia. One of the main issues concerning the dynamics of excess electrons in H-bonded solvents is the spectroscopic consequence of this process. Hydroxyl solvents, amines, and ammonia are among the solvents where the structural properties of the solvating medium compared with its bulk dielectric properties seem to be much more important in determining the spectroscopic properties of the solvated electron.[8,34] Although from the optical spectrum one cannot directly distinguish between a H-bond-oriented or dipole-oriented cavity, a solvated anion, or any other structure, the theoretical models used for interpretation of the experimental absorption spectra of the solvated electron may provide valuable hints about the first solvent shell and the extent of the excess electron density.

In an attempt to elucidate the origin of the optical absorption spectrum of the solvated electron, the following physical concepts have been proposed: (a) the optical absorption band as the envelope of a set of discrete $1s \rightarrow np$ transitions superimposed on bound continuum profiles; (b) statistical distributions of molecular traps; (c) coupling between the electron motion and high- and low-frequency modes of the solvent. The first two groups of theories use the concept of an excess electron localized at a cavity where interactions of the excess electron with the molecular en-

(34) Clark, T.; Illing, G. *J. Am. Chem. Soc.* **1987**, *109*, 1013.
(35) Webster, B. *J. Phys. Chem.* **1980**, *84*, 1070.
(36) Nelson, P. D., Jr.; Klemper, W.; Fraser, G. T.; Lovas, F. J.; Suenram, R. D. *J. Chem. Phys.* **1987**, *87*, 6364.
(37) Lemley, A. T.; Roberts, J. H.; Plowman, K. R.; Lagowski, J. J. *J. Phys. Chem.* **1973**, *77*, 2185.
(38) Yeo, G. A.; Ford, T. A. *THEOCHEM* **1988**, *45*, 247.
(39) Fueki, F.; Feng, D. F.; Kevan, L.; Christofferson, R. *J. Phys. Chem.* **1971**, *75*, 2297.
(40) Kestner, N. R.; Jortner, J. *J. Phys. Chem.* **1984**, *88*, 3818.
(41) Kevan, L. *J. Phys. Chem.* **1981**, *85*, 1628.
(42) Dawes, S. B.; Ward, D. L.; Huang, R. H.; Dye, J. L. *J. Am. Chem. Soc.* **1986**, *108*, 3534.
(43) Symons, M. C. R., Jr. *J. Phys. Chem.* **1988**, *92*, 7260.
(44) Murphy, S. V.; Hilbert, D. B. *Radiat. Phys. Chem.* **1086**, *28*, 1319.
(45) Webster, B. *J. Phys. Chem.* **1975**, *79*, 2809.
(46) Tuttle, T. R., Jr.; Golden, S. *J. Chem. Soc., Faraday Trans. 2* **1979**, *75*, 1146.
(47) Tuttle, T. R., Jr.; Golden, S. *J. Phys. Chem.* **1980**, *84*, 2457.
(48) Tuttle, T. R., Jr.; Golden, S. *J. Chem. Soc., Faraday Trans. 2* **1981**, *77*, 138, 889, 1421.
(49) Tuttle, T. R., Jr.; Golden, S. *J. Chem. Soc., Faraday Trans. 2* **1982**, *78*, 1581.
(50) Golden, S.; Tuttle, T. R., Jr. *J. Phys. Chem.* **1984**, *88*, 3781.
(51) Razem, D.; Hamill, W. H. *J. Phys. Chem.* **1984**, *88*, 488.
(52) Jortner, J. *Mol. Phys.* **1962**, *5*, 257; *J. Chem. Phys.* **1959**, *36*, 839.
(53) Feng, D.-F.; Kevan, L. *Chem. Rev.* **1980**, *80*, 1.
(54) Rao, K.; Kestner, N. R. *J. Chem. Phys.* **1984**, *80*, 1587.
(55) Rossky, P. J.; Schnitker, J. *J. Phys. Chem.* **1988**, *92*, 4277.
(56) Barnett, R. B.; Landman, U.; Nitzan, A. *J. Chem. Phys.* **1989**, *90*, 4413.
(57) Wallqvist, A.; Thirumalai, D.; Berne, B. J. *J. Chem. Phys.* **1987**, *86*, 6404.
(58) Haberland, H.; Ludwight, Ch.; Schinder, H. G.; Worshop, D. R. *J. Chem. Phys.* **1984**, *81*, 3792.
(59) Migus, A.; Ganduel, Y.; Martin, I. L.; Antonetti, A. *Phys. Rev. Lett.* **1987**, *58*, 1559.
(60) Webster, B. C.; Howat, G. *Radiat. Res. Rev.* **1972**, *4*, 259.
(61) Kevan, L. *Adv. Radiat. Chem.* **1974**, *4*, 181.
(62) Holton, D.; Edwards, P. P.; Mc Farlane, W.; Wood, B. *J. Am. Chem. Soc.* **1983**, *105*, 2104.
(63) Kenney-Wallace, G. A.; Jonah, C. D. *J. Phys. Chem.* **1982**, *86*, 2572.
(64) Schniker, J.; Rossky, P. J.; Kenney-Wallace, G. A. *J. Chem. Phys.* **1986**, *85*, 2986.
(65) Funabashi, K.; Carmichael, I.; Hamill, W. H. *J. Chem. Phys.* **1978**, *69*, 2652.
(66) Rentzepis, P. M.; Jones, R. P.; Jortner, J. *J. Chem. Phys.* **1973**, *59*, 766; *Chem. Phys. Lett.* **1972**, *15*, 480.
(67) Walker, D. C. *J. Phys. Chem.* **1980**, *84*, 1140.
(68) Callef, D. F.; Wolynes, P. G. *J. Chem. Phys.* **1983**, *78*, 4145.

vironment are simulated by polarizable point multipoles in semicontinuum models,[53] molecular electron density in ab initio and semiempirical quantum methods,[33,34,54] and long-range electrostatic potentials in continuum models.[69] The third group of theories is based on short-range interactions between the excess electron and the environment where the equilibrium structure is modified by selective attachment to intramolecular vibrational modes of the molecules forming the trap (cavity models) or of the anion on which the electron is imagined to be localized (solvated anion models). In the latter model the additional electron remains external to the neutral molecule, being attached through Rydberg-type orbitals rather than as an additional electron that is incorporated into the molecular density of the neutral molecule. From this selective attachment we can deduce something about the geometry of the cavity or the preferential sites on anions. It seems that in H-bonded solvents the proton donor OH or NH group vibrations, which are sensitive upon H-bond formation, are the accepting modes, implying a strong coupling between the electron and the intramolecular vibrational modes. These physical concepts have been described with the aid of such various theoretical techniques and approaches as linear response theory,[70] adiabatic approximations,[71] or self-consistent field methods.[33] Recently, we have proposed a theoretical model[1] that combines both the ideas of statistical distribution of the traps and coupling to the intramolecular vibrational modes of the solvent. The purpose of the present paper is to examine to what extent the experimental band shapes of solvated electrons in ammonia and amines can be understood in terms of our theory.[1]

Numerical Calculations of the Absorption Band Shape and Results

In the framework of linear response theory, the absorption coefficient is expressed as

$$\epsilon(\omega) = \frac{2\pi\omega}{3\hbar cnV}(1 - \exp(-\beta\hbar\omega)) \int_{-\infty}^{+\infty} \langle M^+(t)\, M(0)\rangle e^{-i\omega t}\, dt \quad (1)$$

where M denotes the dipole moment of the sample, V its volume, and n the refractive index. Recently, we have proposed a theory of absorption spectra of solvated electrons.[1] The theoretical development considers the contribution to the absorption band profile from vibrational coupling, tunneling, and inhomogenous broadening due to the statistical variety of trapping sites. The vibrational coupling includes interaction between the solvated electron and the solvent molecules forming the trap (in terms of the "cavity" or "solvated anion" model). The vibrational coupling is treated in the framework of strong coupling limit theory, where the displacement operator A obtained with aid of a canonical transformation creates dynamic effects between its Born–Oppenheimer eigenstates. The time evolution of the operator A is governed by the Liouville equation for the vibrational density operator of the q mode relaxing to the bath. The coupling between the q mode and the bath is described in terms of resonance energy exchange and is characterized by the dumping parameter Γ. Despite this indirect coupling of the solvated electron to the bath (through the q mode), we can expect direct coupling (in homogeneous broadening). Direct coupling to the bath is responsible for the fluctuations of the potential well (single- or double-well potential) and the electronic energy levels. For equilibrium averaging over these fluctuations we have used the cumulant expansion procedure. The fluctuations of the energy levels (electronic dephasing, characterized by a and τ_a in eq 5) and the fluctuations of the energy potential well (b and τ_b in eq 5) are regarded as random stochastic variables in the two-level system, governed by the stochastic Liouville equation. The origin of the fluctuations of the potential well is due to the assumptions that were introduced in the strong coupling treatment of the electron–vibrational mode coupling: (i) the vibrational frequencies in the ground and excited states of the cavity (or anion) are the same; (ii) only one vibrational mode is modified in the absorption process; and (iii) the equilibrium geometry of the potential well in the excited electronic state is displaced linearly with respect to the normal vibrational coordinate. Generally, these assumptions are not justifiable. Effects (i)–(iii) were formally included in our model by regarding the electronic transition as a transition in the potential well fluctuating with time.

We have shown[1] that the dipole correlation function $\langle M^+(t)\, M(0)\rangle$ is given by

$$\langle M^+(t)\, M(0)\rangle = e^2\epsilon\epsilon_1 \sum_{\gamma=0}^{\infty} \epsilon_2(\gamma) \sum_{m=1}^{4} \Big[\sum_{\alpha=0}^{\gamma} \sum_{j=0}^{\alpha} \sum_{k=0}^{\alpha} \sum_{l=0}^{\infty} \sum_{p=0}^{l} A_{lp\gamma\alpha j} C_{kjl\gamma\alpha} \langle B^m_{\gamma\alpha}\rangle + \sum_{\alpha=\gamma+1}^{\infty} \sum_{j=0}^{\gamma} \sum_{k=0}^{\gamma} \sum_{l=0}^{\infty} \sum_{p=0}^{l} A_{lp\alpha\gamma j} C_{kja\gamma} \langle B^m_{\alpha\gamma}\rangle \Big] \quad (2)$$

where

$$A_{lp\gamma\alpha j} = \binom{l}{p} \frac{\gamma!\alpha!(-1)^{k+j+l}}{2^l(\alpha - k)!(\alpha - j)!(\gamma - \alpha + k)!(\gamma - \alpha + j)!} \quad (3)$$

$$C_{kjl\gamma\alpha} = \alpha_0^{2(k+j+l+\gamma-\alpha)} \quad (4)$$

$$\langle B^m{}_{\gamma\alpha}\rangle = f_m \exp\{-i[\langle\omega_0{}^1\rangle + \langle\omega^{mt}\rangle - 2\alpha_0{}^2\omega_{00} + (\gamma - \alpha)\omega_{00}]t\} \exp\{-[(\gamma - \alpha) + 2p + 2j]\Gamma t/2\} \times \exp\{-2a^2[\tau_a{}^2(\exp(-t/\tau_a) - 1) + \tau_a t]\} \times \exp\{-b^2[\tau_b{}^2(\exp(-t/\tau_b) - 1) + \tau_b t]\} \quad (5)$$

All of the other symbols in eqs 2–5 have been explained in refs 1 and 75. Using eqs 1–5, we have calculated the theoretical spectra for ammonia and amines and compared with experiment. In all cases, summation over γ up to 20 was sufficient in order to achieve convergence in eq 2. The absorption band of the solvated electron in ammonia is observed at 0.897 eV at 200 K.[20] The band is featureless and asymetric with a long tail extending to high frequencies. The asymetry factor W_r/W_b characterizing the ratio of the bandwidths in the red and blue regions is equal to 1.39.[6] The experimental parameters of the bands in ammonia, methylamine, and trimethylamine taken for comparison with theory are given in Table I. In contrast with the other H-bonded solvents, the bandwidths in ammonia and amines are relatively narrow. For comparison, the half-width in methanol is nearly four times, in water nearly two times, broader than in ammonia.[72] To reproduce the absorption bands in ammonia and amines we must turn for a moment to the parameters that have been used in our theory.[1,75] The angular frequency $\langle\omega_0{}^1\rangle$ is the electronic transition frequency of the solvated electron when there is no coupling to the intramolecular vibrational modes of the solvent. This parameter can be treated as the depth of the trap. It was taken as equal to 1.1 eV for ammonia, as obtained from experimental estimations of the solvation energy.[73]

The difference in the solvation energies for monomer anions of ammonia and methylamine was calculated to be 0.0173 eV.[34] Assuming a cavity with six molecules and a linear dependence of solvation energy of the number of solvent molecules, we have used 1.2 eV for methylamine.

The coupling constant α_0, which characterizes the strength of the coupling of the excess electron with the intramolecular vibrational modes of the molecule, is treated as a fitting parameter and is chosen to reproduce the extinction coefficient at the absorption maximum. The dumping parameter Γ reflects the strength of the coupling between the mode and the thermal bath (translational, reorientational degrees of freedom, low-frequency intermolecular vibrational modes of the solvent). We have put Γ at 110 cm^{-1} for ammonia and 200 cm^{-1} for methylamine and trimethylamine, which corresponds to the stretching mode ν_s of the hydrogen bridge NH···N.[74] We have set the a and b pa-

(69) Jortner, J. *Ber. Bunsen-Ges. Phys. Chem.* **1984**, *88*, 188.
(70) Banerjee, A.; Simons, J. *J. Chem. Phys.* **1978**, *68*, 415.
(71) Copeland, D. A.; Kestner, N. R.; Jortner, J. *J. Chem. Phys.* **1970**, *53*, 1189.
(72) Jou, F.-Y.; Freeman, G. R. *J. Phys. Chem.* **1977**, *81*, 909.
(73) Lapoutre, G.; Jortner, J. *J. Phys. Chem.* **1972**, *76*, 53.
(74) Pimentel, G. C.; McClellan, A. L. *The Hydrogen Bond*; Freeman: San Francisco, 1960.

TABLE I: Spectral Properties of e_s^- in Ammonia, Methylamine, and Trimethylamine

solvent	T, K	exptl ν_{max}, eV	theor ν_{max}, eV	exptl $W_{1/2}$, eV	theor $W_{1/2}$, eV	exptl W_b/W_r	theor W_b/W_r	$10^{-4}\epsilon_{max}$, L mol^{-1} cm^{-1}
ammonia	203[a]	0.897[a]	0.868	0.399[a]	0.384	1.39[b]	1.38	4.9 ± 0.1[c]
	200[b]	0.917[b]		0.405[b]				
methylamine	203[a]	0.995[a]	0.942	0.586[a]	0.557			3.3 ± 0.2[c]
trimethylamine	77[d]	0.729[d]	0.750	0.589[d]	0.582			

[a] Reference 20. [b] Reference 6. [c] Reference 11. [d] Reference 83.

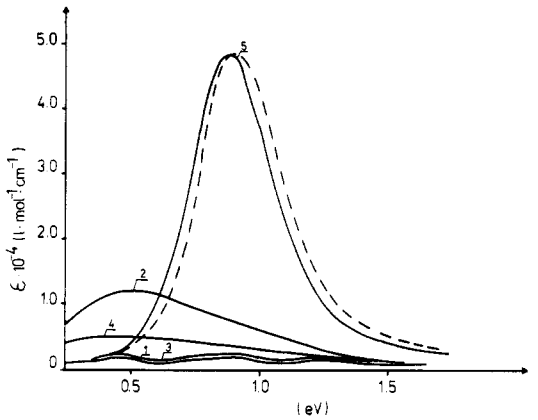

Figure 1. Absorption profiles of an electron solvated in ammonia at 203 K: (–) theory; (- - -) experiment.[6] Parameters: $\langle\omega_0^1\rangle$ = 1.1 eV; Γ = 110 cm^{-1}; α_0 = −2.412; a = 0.0; b = 0.0; (1) ω_{00} = 3298 cm^{-1} (ν_1); (2) ω_{00} = 1070 cm^{-1} (ν_2); (3) ω_{00} = 3380 cm^{-1} (ν_3); (4) ω_{00} = 1658 cm^{-1} (ν_4); (5) ω_{00} = 320 cm^{-1} (ν_t).

rameters equal to zero, which means that the influence of direct coupling to the bath (inhomogeneous broadening) is assumed to be negligible and the Born–Oppenheimer potential well is static with time.

Ammonia has the following normal modes: $\nu_1(A_1)$ symmetric stretching at 3298 cm^{-1}, $\nu_2(A_1)$ symmetric bending at 1070 cm^{-1}, ν_3(E) asymmetric stretching at 3380 cm^{-1}, ν_4(E) asymmetric bending at 1638 cm^{-1}, and the torsional mode at 320 cm^{-1}.[37] In Table I we have shown the experimental parameters characterizing the band shape compared with the theoretical one, which we have obtained from our model.

In Figure 1 we have shown the theoretical spectra calculated from eqs 1–5 for the solvated electron in ammonia coupled with all of the normal modes. We can see that the experimental band[11,16] is very well reproduced only by the torsional mode ν_t. The higher frequency stretching modes ν_1 and ν_3 give negligible contributions to the band intensity. The coupling to the bending modes ν_2 and ν_4 gives a doubled bandwidth, as compared with experiment. There is a similarity in this respect between ammonia and water. Recently, we have shown[75] that the electrron solvated in water is also coupled with the torsional mode ν_t at 720 cm^{-1}. Coupling with the torsional mode is expected to be strongest when NH groups are directed toward the electron in the center because the dipole-oriented or diffuse anion structures are not modified by the torsional mode. Our results for ammonia are in agreement with those obtained from molecular dynamics simulations. Spirik et al.[31] have found that the fluctuations of the adiabatic electronic energy are driven by the molecular librations in the hydrogen-bonded solvent. Their results show that the intensities of the adiabatic fluctuations of the binding energy of the solvated electron in ammonia for frequencies above 400 cm^{-1} are negligible, and thus the electron does not appear to be coupled to the high-frequency intramolecular modes of the solvent, which is in good agreement with the torsional frequency of 320 cm^{-1} in our calculations.

However, the peak position in ammonia obtained from the simulations of Spirik et al. is notably blue shifted with respect to the experimental spectrum, giving a peak position at 1.2 eV. They suggested that this discrepancy arises from an inadequacy

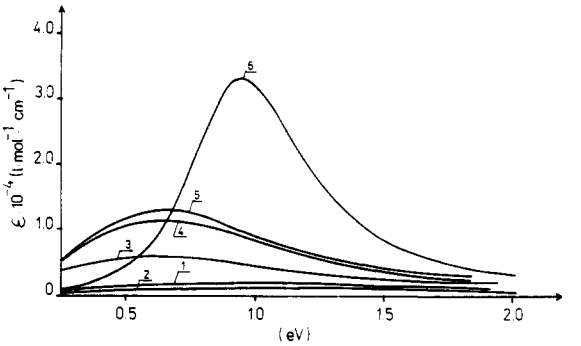

Figure 2. Absorption profiles of an electron solvated in methylamine at 203 K: $\langle\omega_0^1\rangle$ = 1.2 eV; Γ = 200 cm^{-1}; α_0 = −2.415; a = 0.0; b = 0.0; (1) ω_{00} = 3260 cm^{-1} (ν_1); (2) ω_{00} = 3371 cm^{-1} (ν_{10}); (3) ω_{00} = 1622 cm^{-1} (ν_4); (4) ω_{00} = 1040 cm^{-1} (ν_8); (5) ω_{00} = 955 cm^{-1} (ν_9); (6) ω_{00} = 370 cm^{-1} (ν_t).

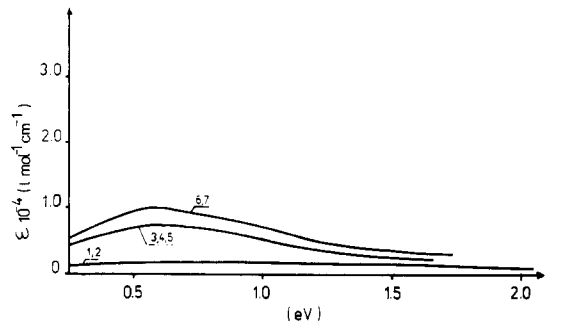

Figure 3. Absorption profiles of an electron solvated in methylamine at 203 K: $\langle\omega_0^1\rangle$ = 1.2 eV; Γ = 200 cm^{-1}; α_0 = −2.415; a = 0.0; b = 0.0; (1) ω_{00} = 2887 cm^{-1} (ν_2); (2) ω_{00} = 2793 cm^{-1} (ν_3); (3) ω_{00} = 1467 cm^{-1} (ν_5); (4) ω_{00} = 1441 cm^{-1} (ν_6); (5) ω_{00} = 1492 cm^{-1} (ν_{12}); (6) ω_{00} = 1182 cm^{-1} (ν_7); (7) ω_{00} = 1172 cm^{-1} (ν_{14}).

of the electron–solvent pseudopotential used in simulations. We think that there is another reason for this discrepancy. The band position obtained from simulation is in surprisingly good agreement with $\langle\omega_0^1\rangle$, characterizing in our model the peak position when there is no vibronic coupling. The simulation employs rigid ammonia molecules and so the possible coupling of the electron to molecular vibrations is completely neglected. Our results support the argument that the electron–solvent potential in Spirik's simulations is good, but the omission of vibronic coupling (inadequate solvent–solvent potential) has this serious effect on the absorption spectrum.

In Figure 2 we have presented the theoretical absorption bands for the electron in methylamine for all of the normal modes.[76-82] Unfortunately, we could not find in the literature the absorption band profile for methylamine for comparison; we found only the parameters characterizing the band such as the peak position, bandwidth, and extinction coefficient. In Table I we compared

(75) Abramczyk, H.; Kroh, J. *J. Phys. Chem.*, in press.

(76) Gray, A. P.; Lord, R. C. *J. Chem. Phys.* **1957**, *26*, 690.
(77) Wolf, H.; Ludwig, H.; *Ber. Bunsen-Ges. Phys. Chem.* **1964**, *68*, 143.
(78) Wolf, H.; Staschewski; D. *Ber. Bunsen-Ges. Phys. Chem.* **1964**, *68*, 135.
(79) Dellephiane, G.; Zerbi, C. *J. Chem. Phys.* **1968**, *48*, 3573.
(80) Wu, E. L.; Zerbi, G.; Califano, S.; Crawford, B., Jr., *J. Chem. Phys.* **1961**, *35*, 2060.
(81) During, J. R.; Bush, S. F.; Baglin, F. G. *J. Chem. Phys.* **1968**, *49*, 2106.
(82) Goldfarb, T. D.; Khare, B. N. *J. Chem. Phys.* **1967**, *46*, 3379.

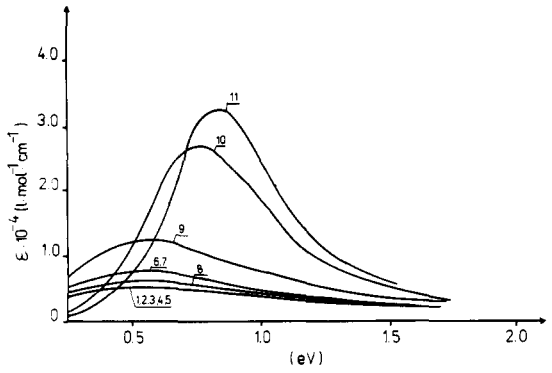

Figure 4. Absorption profiles of an electron solvated in trimethylamine at 77 K: $\langle\omega_0^1\rangle$ = 1 eV; Γ = 200 cm^{-1}; α_0 = −2.405; a = 0.0; b = 0.0; (1) ω_{00} = 1475 cm^{-1} (ν_3); (2) ω_{00} = 1470 cm^{-1} (ν_4); (3) ω_{00} = 1456 cm^{-1} (ν_5); (4) ω_{00} = 1440 cm^{-1} (ν_{16}); (5) ω_{00} = 1405 cm^{-1} (ν_{17}); (6) ω_{00} = 1187 cm^{-1} (ν_5); (7) ω_{00} = 1098 cm^{-1} (ν_{18}); (8) ω_{00} = 1270 cm^{-1} (ν_{20}); (9) ω_{00} = 823 cm^{-1} (ν_6); (10) ω_{00} = 365 cm^{-1} (ν_7); (11) ω_{00} = 259 cm^{-1} (ν_{22}).

the theoretical bandwidth with the experimental one.[11] In Figure 2 we have shown the coupling with normal modes of the NH_2 groups: (a) NH stretch, ν_1 (3260 cm^{-1}), ν_{10} (3371 cm^{-1}); (b) NH deformation, ν_4 (1622 cm^{-1}); (c) CN stretch, ν_0 (1044 cm^{-1}); (d) NH wag, ν_9 (955 cm^{-1}); and (e) NH torsion, ν_{15} (370 cm^{-1}). The coupling with the normal modes associated mainly with the alkyl groups are shown in Figure 3: (a) CH stretch, ν_2 (2887 cm^{-1}), ν_3 (2793 cm^{-1}); (b) CH deformation, ν_5 (1467 cm^{-1}), ν_6 (1441 cm^{-1}) and ν_{12} (1492 cm^{-1}); and (c) CH wag, ν_7 (1182 cm^{-1}), ν_{14} (1172 cm^{-1}).

We can see from Figures 2 and 3 and Table I that coupling with the NH torsional mode at 264 cm^{-1} gives the most intense band and the best agreement with experiment. The theoretical bandwidth is 0.558 eV, while the experimental one is reported as 0.595 eV. All the other modes do not reproduce the band shape, giving bandwidths significantly broader than those observed experimentally. The coupling with modes that have frequencies higher than 1000 cm^{-1} gives negligible intensities. These results practically exclude alkyl groups as the sites of preferential attachment. Our results show that, the same as in ammonia, the electron is coupled with the torsional mode of the NH group, suggesting attachment through the H bonding of N–H···e$^-$ in the cavity. The diffuse anion structure with the electron on nitrogen or the dipole-oriented structure seems to be much less sensitive to the torsional vibration of the NH group. The absorption band of trimethylamine offers a promising example for checking on the role of H-bond interactions in amines with an electron in the cavity. In this case interactions between the electron and vibrational modes through H-bond interactions are eliminated and the NH torsion mode does not exist.

In Figure 4 we have shown the coupling with normal modes of trimethylamine by using argon matrix frequencies and point group C_{3v}:[82] (a) CH deformation, ν_3, ν_4, ν_{15}, ν_{16}, and ν_1^7 at 1475, 1470, 1456, 1440, and 1405 cm^{-1}, respectively; (b) CH rock, ν_5, ν_{18}, and ν_1^9 at 1187, 1098, and 1037 cm^{-1}, respectively; (c) N–C stretch, ν_6 and ν_{20} at 823 and 1270 cm^{-1}, respectively; (d) N–C deformation, ν_{21} at 421 cm^{-1}; (e) C–N–C bend, ν_7 at 365 cm^{-1}; and (f) CH torsion, ν_{22} at 259 cm^{-1}. The best agreement with experiment[83] that we obtained for the C–N–C bending mode was at 365 cm^{-1}, as shown in Table I.

The band calculated for the case of CH torsion is too narrow, the couplings with the other modes make the bands unreasonably broad, as compared with experiment. These results evidently suggest that the electron cannot be localized on nitrogen in the diffuse solvated anion structure and cannot be trapped in the alkyl cavities because in such cases all the modes belonging to the (a)–(f) groups should make a contribution to the bandwidth. Taking into account that the dipole moment of the molecule is particularly sensitive to C–N–C bending, one can suggest that the electron solvated in trimethylamine forms a dipole-oriented cavity. It is worth noticing that we obtained the same type of coupling with a bending mode for alcohols,[75] which are commonly assumed to form dipole-oriented cavities. Our results are in agreement with ab initio results.[34] Clark and Illing have obtained that the H-bond-oriented structure for methylamine is slightly more stable than the dipole-oriented one. They did not study trimethylamine but for ethylamine and dimethylamine have obtained the dipole-oriented structure.

Conclusions

Our model seems to generate the peak position, the width, and the asymmetry of the absorption spectra of solvated electrons in ammonia, methylamine, and trimethylamine with fair accuracy. The absorption spectra in ammonia and methylamine are ascribed to electrons in hydrogen-bond-oriented cavities, while in trimethylamine to electrons in dipole-oriented cavities. The bandwidths arise from the combination of the vibronic bands due to coupling of the electron with the torsional mode ν_t at 320 cm^{-1} for ammonia and 370 cm^{-1} for methylamine and to coupling of the electron with the bending C–N–C mode ν_7 at 365 cm^{-1} for trimethylamine.

The vibronic bands are broadened by the coupling of intramolecular modes ν_t or ν_b with low-frequency modes of the bath. Inhomogeneous broadening due to the distribution of solvent environments plays a minor role. The short-time dynamics probed by the spectral band shape is not affected by tunneling.

Registry No. Ammonia, 7664-41-7; methylamine, 74-89-5; trimethylamine, 75-50-3.

(83) Shida, T.; Iwata, S.; Watanabe, T. *J. Phys. Chem.* **1972**, *76*, 3683.